

Statistical inference on errorfully observed graphs

Carey E. Priebe, Daniel L. Sussman, Minh Tang, and Joshua T. Vogelstein

Johns Hopkins University, Department of Applied Mathematics and Statistics

September 23, 2018

Abstract

Statistical inference on graphs is a burgeoning field in the applied and theoretical statistics communities, as well as throughout the wider world of science, engineering, business, etc. In many applications, we are faced with the reality of errorfully observed graphs. That is, the existence of an edge between two vertices is based on some imperfect assessment. In this paper, we consider a graph $G = (V, E)$. We wish to perform an inference task – the inference task considered here is “vertex classification”, i.e., given a vertex v with unknown label $Y(v)$, we want to infer the label for v based on the graph G and the given labels for some set of vertices in G not containing v . However, we do not observe G ; rather, for each potential edge $uv \in \binom{V}{2}$ we observe an “edge feature” which we use to classify uv as edge/not-edge. Thus we *errorfully* observe G when we observe the graph $\tilde{G} = (V, \tilde{E})$ as the edges in \tilde{E} arise from the classifications of the “edge features”, and are expected to be errorful. Moreover, we face a quantity/quality trade-off regarding the edge features we observe – more informative edge features are more expensive, and hence the number of potential edges that can be assessed decreases with the quality of the edge features. We studied this problem by formulating a quantity/quality trade-off for a simple class of random graphs model, namely the stochastic blockmodel. We then consider a simple but optimal vertex classifier for classifying v and we derive the optimal quantity/quality operating point for subsequence graph inference in the face of this trade-off. The optimal operating points for the quantity/quality trade-off are surprising and illustrate the issue that methods for intermediate tasks should be chosen to maximize performance for the ultimate inference task. Finally, we investigate the quantity/quality tradeoff for errorful observations of the *C. elegans* connectome graph.

1 Introduction

In areas ranging from connectomics, where vertices may be neurons and edges indicate axon-synapse-dendrite connections, to social networks, where vertices may be people and edges indicate communication activity, statistical inference on graphs is becoming essential to scientific, engineering, and business activity. However, in many of these applications edges cannot be directly observed and instead we must infer their existence based on auxillary edge features. This reality gives rise to errorfully observed graphs, and the trade-off between more informative but more expensive edge features and less informative but less expensive edge features is of fundamental interest.

For example, in connectomics, one often observes image data obtained from some spatial scanning procedure, and there is a quantity/quality trade-off between, e.g., spatial resolution of the images and imaging time (higher resolutions requires longer imaging time) or spatial resolution and signal-to-noise ratio (higher resolutions implies lower signal-to-noise ratio per voxel). After the imaging data has been obtained, a tracing algorithm is then employed on the images to infer relationships on the brain-graphs. There is once again a quantity/quality trade-off between how accurate the tracing is and how many images can be traced. As another example, in social network analysis, the edges might have attributes associated with them, e.g., the text of an email or the voice recording of a telephone call. These attributes can be quite complex and so procedures such as topic modeling are commonly used to reduce the edge attribute complexities. These procedures are often computationally demanding and thus there is a trade-off in terms of how accurate one can model the edge attributes and how many edges one can model. See the Appendix for a more detailed summary expounding upon the relevance of the quantity/quality trade-off for these two motivating applications.

We investigate optimal graph inference in the face of this quantity/quality trade-off, and demonstrate that the optimal quantity/quality operating point can be derived for a surrogate graph inference task. In the process, we also demonstrate that the optimal choice of edge-classifier for the subsequent graph inference task is not necessarily the Bayes optimal edge-classifier. We also investigate the quantity/quality tradeoff for simulated errorful observations of the *C. elegans* connectome graph (?). The *C. elegans* is a small worm and the connectome is a representation of the connections between the neurons of the animal as a graph. The connectome provides an abstract wiring diagram for how neuron signals can be passed between neurons in the worm.

1.1 Graph Preliminaries

A graph is a pair $G = (V, E)$ with vertices $V = [n] = \{1, \dots, n\}$ and edges $E \subset \binom{[n]}{2}$. The adjacency matrix A is $n \times n$, binary, symmetric, and hollow, i.e., the diagonal entries of A are all 0; $A_{uv} = 1$ indicates an edge between vertex u and vertex v .

Given a probability space (Ω, P) , a random graph is a graph-valued random variable $\mathbb{G} : \Omega \rightarrow \mathcal{G}_n$, where \mathcal{G}_n denotes the collection of all $2^{\binom{n}{2}}$ possible graphs on $V = [n]$. A random graph model, denoted \mathcal{F} , is some specified collection of distributions on \mathcal{G}_n . We write $\mathbb{G} \sim F_{\mathbb{G}}$ for some distribution $F_{\mathbb{G}} \in \mathcal{F}$.

A simple but interesting random graph model is the stochastic blockmodel, $\mathbb{G} \sim SBM([n], B, \pi)$, introduced in [Holland et al. \(1983\)](#) and of continuing interest ([Airoldi et al. \(2008\)](#); [Snijders and Nowicki \(1997\)](#); [Wang and Wong \(1987\)](#), etc.). Here the block connectivity probabilities are specified via the $K \times K$ symmetric matrix B with $B_{k_1 k_2} \in [0, 1]$, and π in the unit simplex Δ^K specifies the block membership probabilities. Block membership is given by $Y(v) \stackrel{\text{iid}}{\sim} \text{Multinomial}([K], \pi)$, and then $A_{uv} | Y(u), Y(v) \stackrel{\text{ind}}{\sim} \text{Bernoulli}(B_{Y(u), Y(v)})$, yielding independent edges (conditioned on block membership).

The stochastic blockmodel is motivated by the notion of stochastic equivalence and community detection. As the probability of an edge between two nodes depends only on their respective block membership, two nodes sharing the same block membership are stochastically equivalent. Nodes with the same block membership can then be identified as a community, i.e., they share the same communication patterns. Note that in the stochastic blockmodel, the probabilities of a connection within blocks is not necessarily larger than those between blocks. An *affinity* stochastic blockmodel is a stochastic blockmodel wherein the probabilities of connection within a block is in general larger than those between blocks. In an *affinity* stochastic blockmodel, a community is then a collection of nodes whose connections are more dense within the community, as compared to connections between that community and other nodes.

A practically useful and theoretically interesting generalization of the stochastic blockmodel is the latent position model ([Hoff et al., 2002](#)). Consider first fixed latent positions $Z \in \mathbb{R}^{n \times d}$, and $\mathbb{G} \sim LPM(Z, \ell)$ where the link function $\ell : \mathbb{R}^d \times \mathbb{R}^d \rightarrow [0, 1]$. Then $A_{uv} \stackrel{\text{ind}}{\sim} \text{Bernoulli}(\ell(Z_u, Z_v))$. Next, considering random latent positions, we have $\mathbb{G} \sim LPM(F, \ell)$, where $Z \sim F$ on $\mathbb{R}^{n \times d}$ and $A_{uv} | Z_u, Z_v \stackrel{\text{ind}}{\sim} \text{Bernoulli}(\ell(Z_u, Z_v))$, yielding conditionally (on latent positions) independent edges. One of the motivation for latent positions model is the notion of homophily, in which connections between nodes sharing *similar characteristics* are stronger than those between nodes sharing different characteristics. As an example, in a social network with vertices representing individuals and edges indicating communications, the latent position of a vertex

may be interpreted as attributes of the individual in the social space, e.g., interest in various topics. The communication pattern between individuals is then determined by their latent positions and the link function. For example, if the link function is a (monotonic increasing) radial function such as $\exp(-\|Z_u - Z_v\|^2)$, then individuals with attributes that are “close” together are more likely to communicate.

A random dot product graph (RDPG) model (Young and Scheinerman, 2007) is a special case of the latent position model where the link function is the inner product and the latent positions are constrained so that their inner product is always in $[0, 1]$; thus $RDPG(Z) = LPM(Z, \langle \cdot, \cdot \rangle)$ or $RDPG(F) = LPM(F, \langle \cdot, \cdot \rangle)$. We note that, as indicated above, the K -block stochastic blockmodel can be viewed as a special case of a latent positions model where the number of distinct latent positions is K . For example, take F to be the joint distribution for an independent sample of size n from a mixture of d -dimensional Dirichlets: $f_{\text{marginal}} = \sum_{k=1}^K \pi_k D(r_k \vec{\alpha}_k + \vec{1})$. Then let block membership be given by $Y(v) \stackrel{\text{iid}}{\sim} \text{Discrete}([K], \pi)$ and latent positions be given by $Z_v | Y(v) \stackrel{\text{iid}}{\sim} D(r_{Y(v)} \vec{\alpha}_{Y(v)} + \vec{1})$. Finally, let $A_{uv} | Z_u, Z_v \stackrel{\text{iid}}{\sim} \text{Bernoulli}(\langle Z_u, Z_v \rangle)$. This provides a useful *block signal* continuum: when $r_k = 0$ for all k there is no difference among the blocks, while $\min_k r_k \rightarrow \infty$ yields the K -block stochastic blockmodel (when all $\vec{\alpha}_k$ are distinct).

1.2 Inference Preliminaries

Our goal is graph inference. We may wish to cluster vertices, or identify important vertices, or merely perform exploratory data analysis on the graph, looking for interesting structure. For concreteness, we assume that vertices are labeled as belonging to one of K vertex classes (e.g., professors, postdocs, students, etc.) and that we know these vertex class labels for some subset of vertices. In this case, we wish to classify the unlabeled vertices (based on connectivity structure). See Figure 1(left). One common methodology for vertex classification is to embed the graph into finite-dimensional Euclidean space and employ standard classification methodologies. See Figure 1(right).

The embedding depicted in Figure 1 is an adjacency-spectral embedding, the direct embedding of the adjacency matrix A , which is particularly appropriate for the random dot product graph model, as considered in Sussman et al. (2012) and Fishkind et al. (2013). There are many graph embedding techniques, with perhaps the most popular being various instantiations of the Laplacian eigenmap (see, e.g., Belkin and Niyogi (2003)); we shall not be concerned in this paper with the comparative properties of graph embedding techniques. Sussman et al. (2013) demonstrates that $\hat{Z} = \operatorname{argmin}_{Z \in \mathbb{R}^{n \times d}} \|A - ZZ^T\|_F$ admits *universally consistent classification* (Devroye et al., 1996) for random dot product graphs. That is to say, let the rows of $Z \in \mathbb{R}^{n \times d}$ be a collection of (latent) positions, with each row of Z having a class label $k \in \{1, 2, \dots, K\}$.

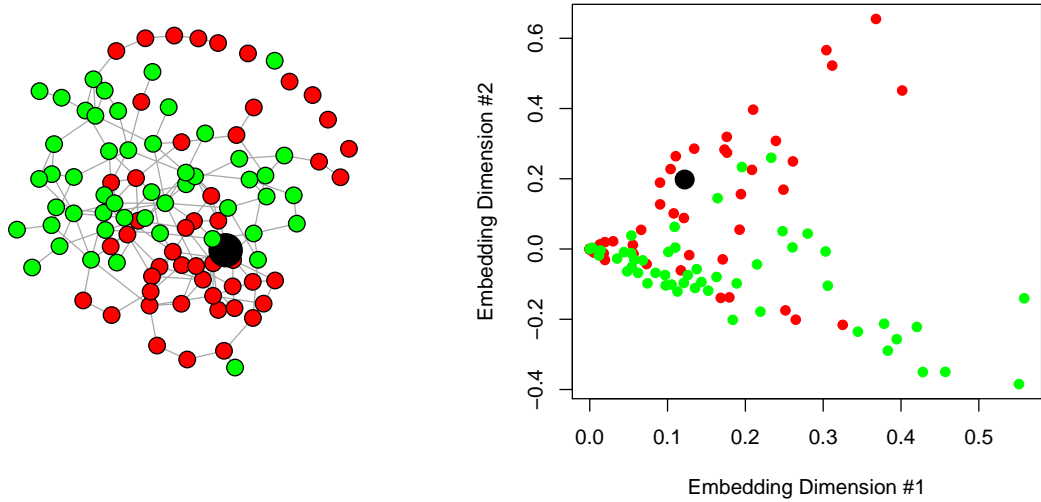


Figure 1: Illustrative graph inference task: *vertex classification*. The graph is a simulated random graph distributed according to the stochastic blockmodel with 100 vertices, see § 1.1. Left Panel: Vertices are labeled as belonging to one of $K = 2$ vertex classes – red and green. We know these vertex class labels for all but one vertex – black. We wish to classify this one unlabeled vertex (based on connectivity structure). Right Panel: Once the vertices are embedded in \mathbb{R}^2 (shown here: adjacency-spectral embedding), the to-be-classified black vertex is easily classified as “red” using a k -nearest-neighbor classifier.

Now let A be the adjacency matrix corresponding to a random dot product graph generated by Z . If we estimate Z by \hat{Z} , then in the limit as $n \rightarrow \infty$ the classification error based on the estimated \hat{Z} can be made as low as the Bayes error rate obtainable when classifying using the true but unobserved Z , for any joint distribution of the latent positions and the class labels.

However, in this paper there are *two* classification tasks to be considered: vertex classification and edge classification. The ultimate goal is graph inference. The *surrogate* inference task considered here is “vertex classification”; that is, we consider vertex class labels $Y(v) \stackrel{\text{iid}}{\sim} \text{Multinomial}([K], \pi)$ and attempt to recover the unobserved vertex class label for distinguished vertex $v^* \in [n]$ based on the observed vertex class labels for $v \in [n] \setminus \{v^*\}$ and the observed graph $G = ([n], E)$. In addition, the errorful nature of our graph observation process induces an edge-classification task; we do not observe E but rather edge features $X(uv)$ for each potential edge $uv \in \binom{[n]}{2}$ from which we must infer E , and subsequent graph inference depends on this edge-classification.

1.3 Outline

In Section 2, we present a model for errorfully observed graphs which admits investigation of the quantity/quality trade-off. Our model for errorfully observed graphs is based on the stochastic blockmodel for random graphs in which edge features are observed rather than edges themselves leading to an edge classification task. In Section 3, we develop the framework for vertex classification, a graph inference task. In Section 4, we demonstrate that the optimal operating point for the quantity/quality trade-off can be identified for our inference task. We also demonstrate the same quantity/quality tradeoff in an investigation of errorful observations of the *C. Elegans* connectome graph. We conclude in Section 5 with a discussion of extensions and implications of this work.

2 Errorfully Observed Graphs

For each potential edge $uv \in \binom{[n]}{2}$ we observe an \mathcal{X} -valued edge feature $X(uv)$. These features may be as complex as “all the information regarding all interactions between actors u and v ” – for instance, electron microscope imagery of axons and dendrites for neurons u and v or the text of all emails twixt addresses u and v . We will assume for simplicity that the X ’s take their values in $[0, 1]$. In both connectomics and social networks, for example, this is often a reasonable assumption: “Peters’ rule” (Braitenberg and Schüz, 1991) suggests that the probability of synapse is proportional to axon/dendrite proximity; topic models (see Blei (2012) for a recent survey) estimate the proportion of topic “sports” (say) for each text document, and then the graph of interest is “who talks to whom about sports.”

Each edge feature $X(uv)$ is associated with the true class label for the potential edge $Y(uv)$. Here, $Y(uv) = 1$ indicates that the edge between vertices u and v is present while $Y(uv) = 0$ indicates its absence. (Note, we will use Y to denote the class label for *both* classification tasks to be considered; it will be easy to distinguish between $Y(v)$, a class label associated with a single vertex, and $Y(uv)$, a class label associated with a pair of vertices, i.e., a potential edge.) The distribution of $X(uv)$ is governed by the value of $Y(uv)$ so that for $Y(uv) = y \in \{0, 1\}$, the class-conditional distributions of the edge features are $F_{X(uv)|Y(uv)=y} = F_y$. Furthermore, we assume the edge features are iid given the presence or absence of an edge so that $X(uv)|Y(uv) = y \stackrel{\text{iid}}{\sim} F_y$. That is, the edge-feature distribution for potential edge uv depends on only $Y(uv)$ (edge /not-edge).

We will assume that the true potential edge class labels $Y(uv)$ are unobserved and instead we only observe the edge features $X(uv)$, so rather than observing the true graph we observe a collection of edge features for

some potential edges. To facilitate subsequent inference, our goal then is to estimate the unobserved true graph by classifying potential edges using the edge features.

For a random graph $\mathbb{G} \sim F_{\mathbb{G}}$, let $\rho = \rho(\mathbb{G}) = \mathbb{E}[|E|/\binom{n}{2}]$ denote the probability that an arbitrary $uv \in \binom{[n]}{2}$ is an edge in the (random) graph; that is, the expected graph density. In this case the edge-feature marginal distribution is $F_X = (1 - \rho)F_0 + \rho F_1$. Without regard to the graph setting and using standard statistical pattern recognition results, we can identify the Bayes edge classifier based on the edge-feature marginal given by $g_{Bayes}(x) = \operatorname{argmax}_{y \in \{0,1\}} P[Y = y | X = x]$. This results in the random graph $\widetilde{\mathbb{G}}_{Bayes}$, whose distribution is induced by $F_{\mathbb{G}}$, F_0 , and F_1 . (NB: Edge classification is not the ultimate goal. Rather, edge classification is an enabling step for subsequent (errorful) graph inference. The optimality of g_{Bayes} for this subsequent inference will be addressed in Section 4.)

We will assume for simplicity that the $[0, 1]$ -valued edge features $X_0 \sim F_0$ and $X_1 \sim F_1$ satisfy the stochastic ordering condition $X_0 <_{ST} X_1$; that is, larger values of the edge feature $X(uv)$ indicate that the potential edge uv is more likely truly an edge. In light of this assumption, we will consider the collection of edge-classifiers given by $g_{\tau}(X) = I\{X > \tau\}$ for threshold $\tau \in [0, 1]$. Note that for the simulation considered in § 4.1, this collection of classifiers includes the Bayes optimal edge classifier.

However, we also have a quantity/quality trade-off: *more informative* edge features are *more expensive*. To capture the idea of our quantity/quality trade-off, we will suppose that there are a collection of class-conditional edge-feature distributions some of which are expensive, so that a meager number of edge features $X(uv)$ will be observed, while others are cheap, so that many or even all of the edge features will be observed. For expensive edge features, the class-conditional distributions are well separated and easy to classify but for cheap edge features the distributions will mostly overlap. If an edge feature for a potential edge is observed we will say that the potential edge has been *assessed*.

We index the collection of class-conditional edge-feature distributions $F_{0,\kappa}, F_{1,\kappa}$ with the *quality* index $\kappa \in (0, \infty)$ such that larger κ implies *more informative but more expensive* edge features. To accommodate the quality/quantity tradeoff, there are natural stochastic ordering conditions: (a) $X_{0,\kappa} <_{ST} X_{1,\kappa}$ for all κ , so that the classifier g_{τ} is reasonable, and (b) $\kappa_1 < \kappa_2$ implies $X_{0,\kappa_1} >_{ST} X_{0,\kappa_2}$ and $X_{1,\kappa_1} <_{ST} X_{1,\kappa_2}$, so that higher quality edge features make classifying potential edges more accurate. Now we introduce the *decreasing quality penalty function* $h : \mathbb{R}_+ \rightarrow [0, 1]$. We actually assess only $100 \cdot h(\kappa)\%$ of the potential edges, so that larger κ implies *more informative but more expensive* edge features and hence fewer potential edges actually classified. We assume that the potential edges not assessed due to the quality penalty $h(\kappa)$ are Missing Completely At Random (MCAR).

We write the collection of potential edges uv as the disjoint union of edges ($uv \in E \iff Y(uv) = 1$) and non-edges ($uv \in \bar{E} \iff Y(uv) = 0$); thus $\binom{[n]}{2} = E \sqcup \bar{E}$. If we denote the set of edges in the estimated graph by \tilde{E} , i.e. the set of potential edges assessed and classified as actual edges, then the event $\{uv \in \tilde{E}\}$ depends on τ through the edge classifier g_τ and on κ and $Y(uv)$ through the class-conditional edge-feature distribution $F_{Y(uv), \kappa}$. Given the class-conditional edge-feature distributions $F_{0, \kappa}$ and $F_{1, \kappa}$ and $\tau \in [0, 1]$, the probability that a potential edge that is truly an edge is assessed and correctly classified as an edge is

$$P_{\tau, \kappa} \left[uv \in \tilde{E} \mid uv \text{ assessed and } uv \in E \right] = 1 - F_{1, \kappa}(\tau).$$

Similarly, the probability that a potential edge that is truly not an edge is incorrectly classified as an edge is

$$P_{\tau, \kappa} \left[uv \in \tilde{E} \mid uv \text{ assessed and } uv \in \bar{E} \right] = 1 - F_{0, \kappa}(\tau).$$

We must also account for the quality penalty $h : (0, \infty) \rightarrow [0, 1]$, decreasing for $\kappa \in (0, \infty)$. Incorporating this penalty, we have $P_{\tau, \kappa}[uv \in \tilde{E} \mid uv \in E] = h(\kappa)(1 - F_{1, \kappa}(\tau))$ and $P_{\tau, \kappa}[uv \in \tilde{E} \mid uv \in \bar{E}] = h(\kappa)(1 - F_{0, \kappa}(\tau))$. Additionally, we choose to set non-assessed potential edges to be non-edges in the final graph, see below and § 5.4.

This framework results in the following *errorfully observed stochastic blockmodel*. Assume that the true underlying graph $\mathbb{G} \sim SBM([n], B, \pi)$ (see §1.1). Using the simple results in the previous paragraph, we define

$$\tilde{B} = h(\kappa) [(1 - F_{1, \kappa}(\tau))B + (1 - F_{0, \kappa}(\tau))(J - B)], \quad (1)$$

where J is the $K \times K$ matrix of all 1's. The resultant *errorfully observed graph distribution*, i.e. the distribution of the graph constructed by assessing and classifying a subset of the potential edges, is given by $\tilde{\mathbb{G}} \sim SBM([n], \tilde{B}, \pi)$. Based on Eq. (1), $h(\kappa)$ can be viewed as the probability that a potential edge is assessed and $1 - F_{1, \kappa}(\tau)$ and $1 - F_{0, \kappa}(\tau)$ are the true and false positive rates, respectively, for the edge classification task, which is only performed on assessed edges.

Another interpretation of the errorful graph model $\tilde{\mathbb{G}} \sim SBM([n], \tilde{B}, \pi)$ is as follows. We start with an unobserved random graph $\mathbb{G} = (V, E)$ distributed according to the stochastic blockmodel with parameters B and π . Based on a selected quality index $\kappa \in (0, \infty)$, for each potential edge uv , an edge feature $X(uv)$, distributed according to $F_{1, \kappa}$ if $uv \in E$ or $F_{0, \kappa}$ if $uv \notin E$, is generated. Let \mathbb{G}_f be the collection of all edge features for each potential, not all of which will be observed. From \mathbb{G}_f , we observe a random subset of the edge features for the assessed potential edges and classify the potential edges as edges and non-edges via some classification rule g that depends on the parameter τ (with the remaining edge features being automatically classified as non-edges). The number of assessed potential edges can be viewed as a binomial random variable

with $\binom{n}{2}$ trials and success probability $h(\kappa)$. The graph $\tilde{\mathbb{G}}$ resulting from the edge classifier on the assessed potential edges is the starting point for our vertex classifier and corresponds to the stochastic blockmodel with parameters \tilde{B} and π as defined in Eq. (1). Note that $\tilde{\mathbb{G}}$ and \tilde{B} will always depend, implicitly, on κ and τ . This formulation assumes that the potential edges that are not assessed, due to the quality penalty $h(\kappa)$, are set to 0 – i.e., non-edge. This choice of dealing with missing values for the potential edges will be revisited later in § 5.4.

Regarding the edge features, our assumption that they are in the interval $[0, 1]$ is for ease of exposition only. In general, the features can take values in any arbitrary space, provided that a reasonable notion/interpretation for stochastic ordering exists in that space. For example, the features can take values in \mathbb{R}^k . One can then classify a potential edge e as an edge if the corresponding feature has value in some subset $S \subset \mathbb{R}^d$. S will then serve the role similar to that of τ in our current setup. The notion of stochastic ordering then corresponds to the notion that the $F_{0,\kappa}(S) \leq F_{1,\kappa}(S)$ for any κ , and that for $\kappa < \kappa'$, $F_{0,\kappa'}(S) \leq F_{0,\kappa}(S) \leq F_{1,\kappa}(S) \leq F_{1,\kappa'}(S)$.

Finally, there is the issue of using an edge classifier to classify the assessed potential edges before performing vertex classification versus working directly with the edge features. That is to say, instead of enforcing dichotomous edge relationships when performing vertex classification, one can try to explicitly model the edge features themselves. We will address this in more detail in the next section, but for now, we remark that the issue of quantity/quality trade-off, as induced by the quality index κ and the penalty function $h(\kappa)$, is independent of our imposition of edge classification as an intermediary inference task.

3 Vertex Classification

Given a graph $G = ([n], E)$ with vertex class labels $Y(v) \in [K]$, there are many methodologies available for estimating the unobserved vertex class label for a distinguished vertex $v^* \in [n]$ based on the observed vertex class labels for $v \in [n] \setminus \{v^*\}$ (recall Figure 1). We will proceed with perhaps the simplest nontrivial vertex classification approach; later, we will see that we can optimize this classifier for τ and κ in the errorfully observed stochastic blockmodel. Briefly, each vertex v is classified as belonging to the block such that v is most likely to be adjacent to vertices in that block.

First, for each $k \in [K]$, we count the number of class k vertices $n_k = \sum_{v \in [n] \setminus \{v^*\}} I\{Y(v) = k\}$. Next, we calculate the k -degree of v^* – the number of class k vertices that are connected to v^* – given by $d_k(v^*) = \sum_{v \in [n] \setminus \{v^*\}} I\{Y(v) = k\} \cdot I\{vv^* \in E\}$. Finally, we classify v^* via $\gamma(v^*) = \operatorname{argmax}_k d_k(v^*)/n_k$.

The classifier γ makes perfect sense for an *affinity* stochastic blockmodel – that is, a stochastic blockmodel with $B_{kk} > B_{kk'}$ for each k and for all $k' \neq k$: assume that $\mathbb{G} \sim SBM([n], B, \pi)$ with B satisfying the affinity conditions and that v^* is chosen uniformly at random, and see that $D_k(v^*)/N_k \approx B_{kY(v^*)}$. Here we have written $D_k(v^*)$ and N_k for the random variable versions of $d_k(v^*)$ and n_k defined above.

In fact, γ is even the Bayes-optimal classifier in our 2×2 setting for B with $B_{11} = B_{22}$, $B_{12} = B_{21} < B_{11}$ and $n_1 = n_2$. Indeed, under this setting, the simple vertex classifier corresponds to the likelihood ratio test. This can be seen as follows. For this model, since the block membership probabilities are equal, the Bayes classifier for classifying a vertex v as class 1 or 2 depends on whether the likelihood ratio

$$\frac{\binom{n_1}{D_1(v^*)} B_{11}^{D_1(v^*)} (1 - B_{11})^{n_1 - D_1(v^*)} \binom{n_2}{D_2(v^*)} B_{12}^{D_2(v^*)} (1 - B_{12})^{n_2 - D_2(v^*)}}{\binom{n_1}{D_1(v^*)} B_{21}^{D_1(v^*)} (1 - B_{21})^{n_1 - D_1(v^*)} \binom{n_2}{D_2(v^*)} B_{22}^{D_2(v^*)} (1 - B_{22})^{n_2 - D_2(v^*)}}$$

is greater than or less than 1, where $D_1(v^*)$ is the number of vertices in class 1 adjacent to v^* and $D_2(v^*)$ is the number of vertices in class 2 adjacency to v^* . Some algebraic simplifications lead to checking whether

$$\left(\frac{B_{11}}{B_{12}}\right)^{D_1(v^*) - D_2(v^*)} \left(\frac{1 - B_{12}}{1 - B_{11}}\right)^{D_1(v^*) - D_2(v^*)}$$

is greater than or less than 1. This is equivalent to checking whether $D_1(v^*) \geq D_2(v^*)$ as $B_{11} > B_{12}$ implies $1 - B_{11} \leq 1 - B_{12}$.

Define $L = P[\gamma(v^*) \neq Y(v^*) | \mathbb{G}, \{Y(v)\}_{v \in [n] \setminus \{v^*\}}]$ to be the probability of misclassifying vertex v^* using classifier γ (Devroye et al., 1996). A simple conditioning argument yields the following result.

Theorem 1. *Let $\mathbb{G} \sim SBM([n], B, \pi)$ be an affinity stochastic blockmodel graph. Let the classifier $\gamma(v^*) = \operatorname{argmax}_k D_k(v^*)/N_k$. Conditional on $[N_1, \dots, N_K] = [n_1, \dots, n_K]$ and $Y(v^*) = k$, the binomials $D_1(v^*) \sim \operatorname{Bin}(n_1, B_{k1})$, \dots , $D_K(v^*) \sim \operatorname{Bin}(n_K, B_{kK})$ are independent. Thus the probability of misclassification with no ties in the classification rule is given by $P[D_k/n_k < \max_{k' \neq k} \operatorname{Bin}(n_{k'}, B_{kk'})/n_{k'}]$; the probability of misclassification in the case of ties, given by T_k , depends on the tie-breaking procedure. Therefore, the probability of misclassification is given by*

$$\begin{aligned} L &= P[\gamma(v^*) \neq Y(v^*) | \mathbb{G}, \{Y(v)\}_{v \in [n] \setminus \{v^*\}}] \\ &= \sum_{\mathcal{S}} \binom{n-1}{n_1, \dots, n_K} \prod_{k=1}^K \pi_k^{n_k} \sum_{k=1}^K \pi_k \left(P \left[\frac{\operatorname{Bin}(n_k, B_{kk})}{n_k} < \max_{k' \neq k} \frac{\operatorname{Bin}(n_{k'}, B_{kk'})}{n_{k'}} \right] + T_k \right) \end{aligned} \quad (2)$$

where the first summation with subscript \mathcal{S} , for the multinomial, is over all non-negative integer partitions of $n-1$ into $[n_1, \dots, n_K]$. (The convention $\frac{0}{0} = 0$ must be adopted for the cases in which some n_k are 0.)

Note that in Theorem 1 we assume that the stochastic blockmodel graph \mathbb{G} is perfectly observed and so τ and κ do not enter in to the calculations. In the next section we optimize the classifier γ for τ and κ in the errorfully observed affinity stochastic blockmodel.

We now remark on our setup where we classify the potential edges into edges and non-edges based on the edge features. It is possible, and even perfectly reasonable, to explicitly model the edge features instead of classifying or assuming a dichotomous edge relationship as we do in this paper. Furthermore, assuming that our model for the edge features is accurate, it is also possible to identify the Bayes optimal vertex classifier. Suppose that for the to-be-classified vertex v^* , we observe m_k edge features for potential edges from v^* to vertices in block k . Denote, these edge features by $X = \{X_i^{(k)} : k \in [K], i \in [m_k]\}$. Given B , π and densities for edge features $f_{1,\kappa}$ and non-edge features $f_{0,\kappa}$, the optimal vertex classifier is given by

$$\begin{aligned} g^*(X) &= \operatorname{argmax}_{y \in [K]} P[Y(v^*) = y | X] \\ &= \operatorname{argmax}_{y \in [K]} \pi_y \prod_{k=1}^K \prod_{i=1}^{m_k} \left(B_{yk} f_{1,\kappa}(X_i^{(k)}) + (1 - B_{yk}) f_{0,\kappa}(X_i^{(k)}) \right). \end{aligned}$$

Note that even using this Bayes optimal vertex classifier we experience a quality/quantity trade-off. Indeed, as we increase κ , the quality of the edge features increases so that the difference between $f_{0,\kappa}$ and $f_{1,\kappa}$ increases. On the other hand the number of observed edge features will decrease, so that m_k will decrease. Finding the optimal quality/quantity trade-off in this case, which is parametrized by only κ , is also of interest.

However, in many realistic situations it will not be possible to observe the edge features directly and we will only have access to pre-classified edge features. In this situation, in addition to κ , there will also be a parameter τ indexing the classification of the edge features. In addition, κ and τ must be chosen in advance. In the example of tracing connections between neurons in the brain this corresponds to pre-selecting a threshold for the tracer stopping criterion. If no such threshold is selected in advance, it is not clear how edge features would be represented. Hence, even though the classifier g^* has minimal error rate and so by the information processing inequality will perform at least as well as the simple classifier γ , we choose to investigate the simpler classifier in order to understand inference in these realistic scenarios. That is to say, the dichotomous nature of our edge classification is but a simplifying notion but we believe that whether we make this simplification or not, the quantity/quality trade-off phenomena to be demonstrated in the next section will be present. We can therefore assume that they are dichotomous without affecting the core message of this paper.

4 Optimizing the Quantity/Quality Trade-Off

Let $\tilde{\mathbb{G}} \sim SBM([n], \tilde{B}, \pi)$ be the errorfully observed graph after edge assessment and classification as defined in Section 2. Recall that the distribution of $\tilde{\mathbb{G}}$ depends on the original block connectivity probability matrix B and on κ and τ (and hence on the quality penalty function h and on the class-conditional edge-feature distributions $F_{0,\kappa}$ and $F_{1,\kappa}$), although this has been suppressed notationally. Notice also that if $SBM([n], B, \pi)$ is an affinity stochastic blockmodel graph, then so is $SBM([n], \tilde{B}, \pi)$, because the edge-feature distribution for potential edge uv depends on only $Y(uv)$ (edge/not-edge) and *does not otherwise depend on the block memberships $Y(u)$ and $Y(v)$* .

Define $L_{\kappa,\tau} = P[\gamma(v^*) \neq Y(v^*) | \tilde{\mathbb{G}}, \{Y(v)\}_{v \in [n] \setminus \{v^*\}}]$ to be the probability of misclassifying vertex v^* using classifier γ for $\tilde{\mathbb{G}}$ with a fixed κ and τ . Eq. (2) applies, replacing the binomial parameters $B_{k_1 k_2}$ with $\tilde{B}_{k_1 k_2}$. Thus the optimal (quality penalty parameter κ , edge-classification threshold τ) pair for the subsequent vertex classification graph inference problem using classifier γ is given by

$$(\kappa^*, \tau^*) = \underset{\kappa, \tau}{\operatorname{argmin}} \sum_{\mathcal{J}} \binom{n-1}{n_1, \dots, n_K} \prod_{k=1}^K \pi_k^{n_k} \sum_{k=1}^K \pi_k \left(P \left[\frac{\operatorname{Bin}(n_k, \tilde{B}_{kk})}{n_k} < \max_{k' \neq k} \frac{\operatorname{Bin}(n_{k'}, \tilde{B}_{kk'})}{n_{k'}} \right] + T_k \right), \quad (3)$$

where we recall the implicit dependence of \tilde{B} on κ and τ (see Eq. (1)). For the purpose of this paper we do not propose methodology to find the optimal pair (κ^*, τ^*) in Eq (3). In the next section we find an approximate optimal solution via grid search.

4.1 Demonstration

Here we present a simple but illustrative demonstration of finding the minimizer in Eq. (3) and the inherent trade-offs of our model. Let $SBM([n], B, \pi)$ be a stochastic blockmodel with $K = 2$, $\pi = [1/2, 1/2]'$ and B satisfying $1 > B_{11} = B_{22} > B_{12} = B_{21} > 0$. Note that B satisfies the affinity SBM conditions. We let the class-conditional edge-features be governed by Beta distributions: $F_{0,\kappa} = \beta_{2,\kappa}$ and $F_{1,\kappa} = \beta_{\kappa,2}$. Our choice of a $F_{0,\kappa}$ and $F_{1,\kappa}$ is primarily to provide a simple illustrative example and because for $\kappa \in (2, \infty)$ these distributions satisfy our stochastic ordering conditions, and that $\kappa = 2$ yields useless features and larger κ yields more informative features. The particular choice of edge features distributions is relevant only in their subsequent impact on the probabilities of error and further down the line the resulting matrix of edge probabilities \tilde{B} . Our choice of Beta distributions provides one possible sweep of these parameters that illustrate the quantity/quality tradeoff phenomenon.

Recall that the collection of edge-classifiers considered is given by $g_\tau(X) = I\{X > \tau\}$ for $\tau \in [0, 1]$, and notice that $\pi = [1/2, 1/2]$ and B doubly stochastic implies that the expected graph density $\rho(\mathbb{G}) = (n\pi^T B\pi - 1^T \text{diag}(B)\pi)/(n-1) = ((n/2) - O(1))/(n-1) \approx 1/2$ and hence, since $f_{0,\kappa}$ and $f_{1,\kappa}$ are reflections about 1/2 of one another, $\tau_{Bayes} \approx 1/2$ for all κ . The quality penalty function considered is $h(\kappa) = (2/\kappa)^3$, so $\kappa = 2$ yields classification of all edges, and while larger κ yields more informative edge features, fewer edges are actually classified. We consider $\tilde{\mathbb{G}} \sim SBM([n], \tilde{B}, \pi)$ to be the associated errorfully observed graph (again, depending on κ and τ). For further simplicity we condition on $N_1 = N_2 = (n-1)/2$.

For this demonstration the classifier γ simplifies, yielding

$$\gamma(v^*) = \underset{k}{\operatorname{argmax}} D_k(v^*) = 1 + I\{D_2(v^*) > D_1(v^*)\} \quad (4)$$

with $D_k(v^*) \stackrel{\text{ind}}{\sim} \text{Bin}(n_k, \tilde{B}_{Y(v^*),k})$. We can simplify the probability of misclassification error rate $L_{\kappa,\tau}$ by noting that by conditioning on $N_1 = N_2$, the first sum in Eq. (1) degenerates into a single summand leaving only the inner sum. Furthermore, using $\pi_1 = \pi_2$ and $\tilde{B}_{1,1} = \tilde{B}_{2,2}$, the probability of misclassification $L_{\kappa,\tau}$ simplifies to

$$\begin{aligned} L_{\kappa,\tau} &= \sum_{k=1}^K \pi_k \left(P \left[\frac{\text{Bin}(n_k, \tilde{B}_{kk})}{n_k} < \max_{k' \neq k} \frac{\text{Bin}(n_{k'}, \tilde{B}_{kk'})}{n_{k'}} \right] + T_k \right) \\ &= P \left[\frac{\text{Bin}(n_1, \tilde{B}_{11})}{n_1} < \frac{\text{Bin}(n_2, \tilde{B}_{12})}{n_2} \right] + (1/2) P \left[\frac{\text{Bin}(n_1, \tilde{B}_{11})}{n_1} = \frac{\text{Bin}(n_2, \tilde{B}_{12})}{n_2} \right] \\ &= \sum_{i=1}^{n_1} P \left[\text{Bin}(n_1, \tilde{B}_{11}) < i, \text{Bin}(n_2, \tilde{B}_{12}) = i \right] + (1/2) P \left[\text{Bin}(n_1, \tilde{B}_{11}) = i, \text{Bin}(n_2, \tilde{B}_{12}) = i \right] \\ &= \sum_{i=1}^{n_1} f_{\text{Bin}}(i; n_1, \tilde{B}_{1,2}) F_{\text{Bin}}(i-1; n_1, \tilde{B}_{1,1}) + (1/2) \sum_{i=0}^{n_1} f_{\text{Bin}}(i; n_1, \tilde{B}_{1,2}) f_{\text{Bin}}(i; n_1, \tilde{B}_{1,1}). \end{aligned} \quad (5)$$

Here, with $K = 2$ and conditioning on $N_1 = N_2$, the sensible tie-breaking procedure “flip a fair coin” is explicitly accounted for in the second sum in our expression for $L_{\kappa,\tau}$.

Figure 2 depicts the error surface $L_{\kappa,\tau}$ for this demonstration, with $n = 51$, $B_{11} = B_{22} = 0.9$ and $B_{12} = B_{21} = 0.1$. The z -axis – probability of misclassification $L \in [0, 1]$, depicted via color and level curves – represents performance on our vertex classification task computed using Eq. (5). The y -axis – $\tau \in [0, 1]$ – represents the threshold for the edge classifier used to obtain \tilde{E} . The x -axis – $h(\kappa) \in [0, 1]$ – represents the proportion of assessed edges as a function of the quality $\kappa \in [2, \infty]$ of the edge-features we observe – larger κ implies *more informative but more expensive* edge-features and hence fewer potential edges actually classified. For this case, $(\kappa^*, \tau^*) \approx (3.5, 0.6)$ and $L_{\kappa^*, \tau^*} \approx 0.161$.

The figure represents this quantity/quality trade-off, and also demonstrates that the optimal choice of edge classifier is *not* the Bayes optimal classifier ($\tau_{Bayes} \approx 1/2$ for all κ). Indeed, using τ_{Bayes} rather than

τ^* results in a substantial relative performance degradation of more than 10%, from $L_{\kappa^*, \tau^*} \approx 0.16$ to $\min_{\kappa} L_{\kappa, \tau_{Bayes}} \approx 0.18$.

Figure 3 and 4 explain this phenomenon by examining the $(\tilde{B}_{1,2}, \tilde{B}_{1,1})$ -path for fixed $\kappa = \kappa^*$ as τ varies from 0 to 1. In Figure 3, we plot the values of $(\tilde{B}_{1,2}, \tilde{B}_{1,1})$ as τ varies. Again, the z -axis, depicted with color and level curves, represents the error rate for the vertex classification task as a function \tilde{B} , as in Eq. (5), rather than pulling back to the $(h(\kappa), \tau)$ coordinates as was done in Figure 2. This figure shows how the particular stochastic blockmodel parameters \tilde{B} for the observed graph impacts performance for the vertex classification task and in comparison to how \tilde{B} varies as a function of τ .

In Figure 4, we plot the mean and variance of $\frac{1}{n}(Z_{1,\tau} - Z_{2,\tau})$ where $Z_{1,\tau} \sim \text{Bin}(n, \tilde{B}_{1,1})$ and $Z_{2,\tau} \sim \text{Bin}(n, \tilde{B}_{1,2})$ as τ varies. Figure 4 indicates that while the mean of $Z_{1,\tau} - Z_{2,\tau}$ is unimodal on $[0, 1]$ with its largest value at $\tau = \frac{1}{2}$, the variance of $Z_{1,\tau} - Z_{2,\tau}$ is monotonically decreasing in τ . If we consider the terms $1 - F_{1,\kappa}$ and $1 - F_{0,\kappa}$ in Eq. (1) as being mixture coefficients for the matrix of true edges and the matrix of false edges, then $\frac{1 - F_{1,\kappa}(\tau)}{1 - F_{0,\kappa}(\tau)}$ increases as τ increases. That is, even though $\tau = 1/2$ might be the Bayes-optimal edge classifier for discerning edges, it turns out that for larger τ , the ratio of true edges among potential edges (vertex pairs) that are labeled edges also increases. Put another way, for $\tau = 1/2$, the absolute difference between the number of true edges and the number of false edges is maximized while for $\tau > 1/2$, though the number of total edges is smaller, the ratio of true edges to false edges is larger.

4.2 Example: *C. elegans* Connectome

As a further illustration of the quality/quantity trade-off for errorfully observed graphs, we will investigate this phenomenon for the *Caenorhabditis elegans* connectome (Varshney et al., 2011; White et al., 1986; ?). The *C. elegans* is a small worm and the connectome is a representation of the connections among neurons in an animal as a graph (see Appendix). The *C. elegans* connectome consists of 302 neurons of which 279 are non-isolate somatic neurons which will be the focus of this investigation. Two different types of connections between neurons are present in the connectome, gap junction synapses and chemical synapses, both of which form weighted connections. We study the gap junction connectome which forms an undirected graph and for simplicity we binarize the edges based on whether the weight of the connection is zero or non-zero. The 279 vertices can be divided into three classes: 118 are sensory neurons, 83 are interneurons, and 78 are motor neurons. Hence, we will study a graph with 279 vertices and 514 edges, giving overall density $\rho = 0.013$. A depiction of the adjacency matrix for this graph is provided in Figure 5.

Using the neuron class labels as the block membership function, we estimated the parameters for a stochastic

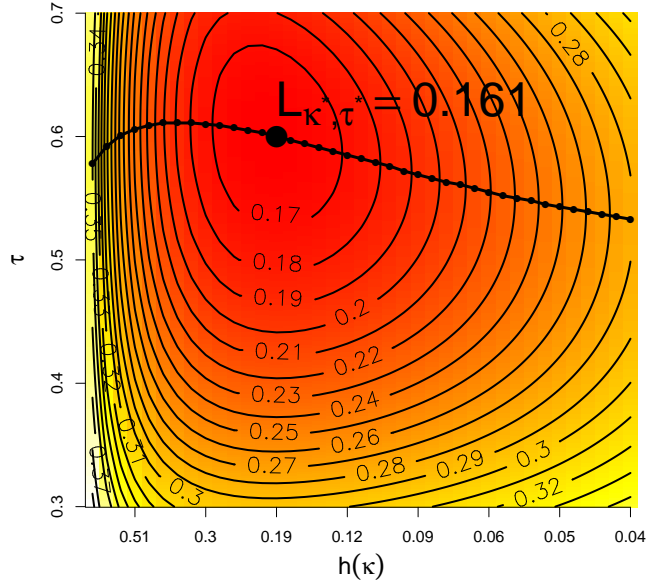


Figure 2: Demonstration of optimal inference for errorfully observed graphs: $(\kappa^*, \tau^*) \approx (3.5, 0.6)$ and $L_{\kappa^*, \tau^*} \approx 0.161$. See Section 4.1 for details. The color and level curves indicate the error rate for the vertex classification task as specified in Eq. (5) with the relationship between \tilde{B} there and τ and $h(\kappa)$ being specified in Eq. (1). The model parameters for the original SBM are $n = 51$, $n_1 = 25 = n_2$, $B_{11} = B_{22} = 0.9$ and $B_{12} = B_{21} = 0.1$. The dotted black curve indicates the optimal classification threshold τ for each $h(\kappa)$, ie for each κ .

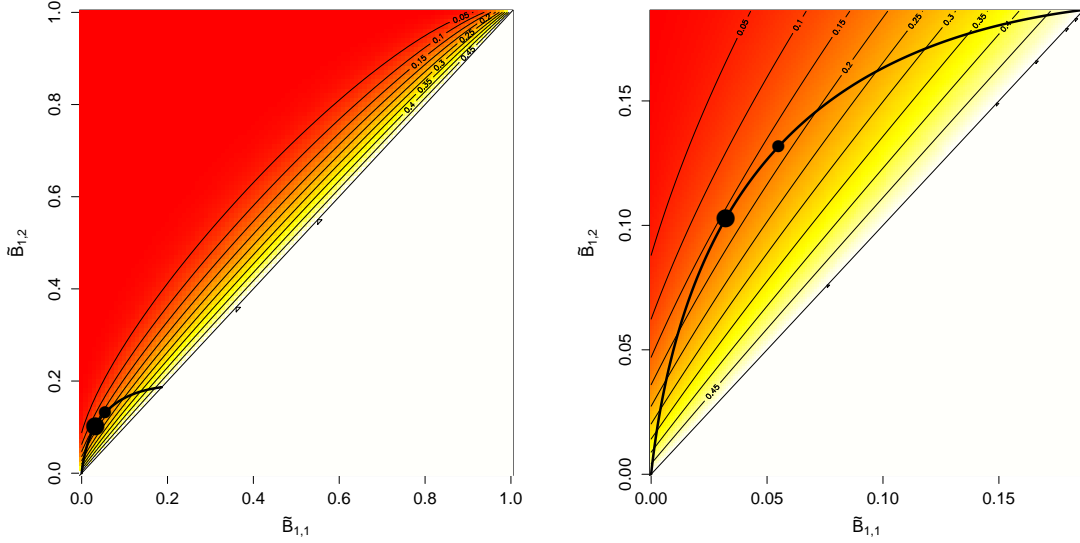


Figure 3: This figure transforms Figure 2 to show $L_{\kappa, \tau}$ as a function of \tilde{B}_{11} and \tilde{B}_{12} . Again, the color and level curves indicate the error rate for the vertex classification task as defined in Eq. (5) as a function of \tilde{B}_{11} and \tilde{B}_{12} . This figure shows the error rate in the $\tilde{B}_{11}, \tilde{B}_{12}$ coordinates directly. The black path shows how $(\tilde{B}_{11}, \tilde{B}_{12})$, whose explicit dependence on κ, τ is given by Eq. (1), vary as τ varies from 0 to 1 for fixed $\kappa = \kappa^* = 3.5$. The axes represent possible edge presence probabilities for the two blocks in the errorfully observed graph which are also the possible parameter values for the two binomials in the simplified expression for $L_{\kappa, \tau}$ (see Eq. (5)). The color and level curves represent $L_{\kappa, \tau}$. The left panel is the full parameter space; the right panel is a zoom-in of the $(\tilde{B}_{12}, \tilde{B}_{11})$ -path. This figure illustrates why the optimal τ^* (the big black dot) $\neq \tau_{Bayes}$ (the little black dot): the curvature of the $(\tilde{B}_{11}, \tilde{B}_{12})$ -path does not match the curvature of the level curves of $L_{\kappa, \tau}$.

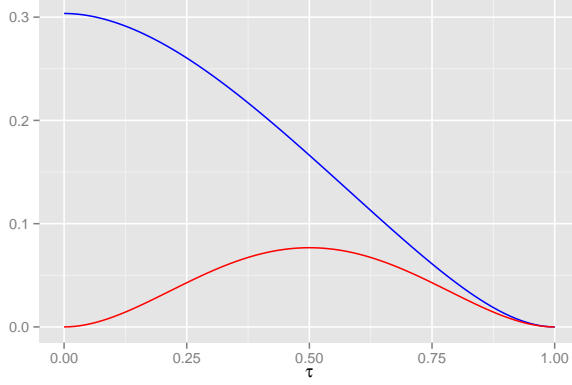


Figure 4: Mean (red curve) and variance (blue curve) of $\frac{1}{n}(Z_{1,\tau} - Z_{2,\tau})$ where $Z_{1,\tau} \sim \text{Bin}(n, \tilde{B}_{11})$ and $Z_{2,\tau} \sim \text{Bin}(n, \tilde{B}_{12})$ as τ varies in $[0, 1]$. $Z_{1,\tau} - Z_{2,\tau}$ corresponds to $D_1(v^*) - D_2(v^*)$ for the simple vertex classifier γ . This figure provides another illustration for why $\tau^* \neq \tau_{Bayes} = 1/2$.

blockmodel with three blocks giving

$$\hat{B} = \begin{bmatrix} 0.015 & 0.017 & 0.002 \\ 0.017 & 0.027 & 0.012 \\ 0.002 & 0.012 & 0.011 \end{bmatrix} \text{ and } \hat{\pi} = [0.42, 0.29, 0.27]'$$

Given estimates \hat{B} and $\hat{\pi}$ we can construct the Bayes plug-in vertex classifier given by

$$g(v^*) = \underset{k \in [3]}{\operatorname{argmax}} \hat{\pi}_k \prod_{k'=1}^3 \text{Bin}(d_{k'}(v^*); n_{k'}, \hat{B}_{kk'}) \quad (6)$$

where v^* is the to-be-classified vertex and $n_k = |\{v \in V \setminus \{v^*\} : Y(v) = k\}|$ for $k = 1, 2, 3$. As our gold standard we computed the leave-one-out error estimate in the case that the whole graph is observed giving an error rate of 0.387.

For this data we do not have formal edge features $X(uv)$ but instead sample an errorfully observed version of the true graph by simulating the impact of choosing κ and τ . As in our simulation example, the exact nature of the edge features and the edge classifier impact the subsequent graph inference only through their impact on the edge assessment probability and the edge classification accuracy. The result of selection of κ and τ given the function h can be distilled as selecting two parameters: the edge assessment probability which determines the probability we will assess the edge features for a particular potential edge and is given by $h(\kappa)$, and the edge classification accuracy, the probability that the assessment will be correct which is a function of κ and τ . Each value of q represents a fixed cost curve for the graph observation procedure where

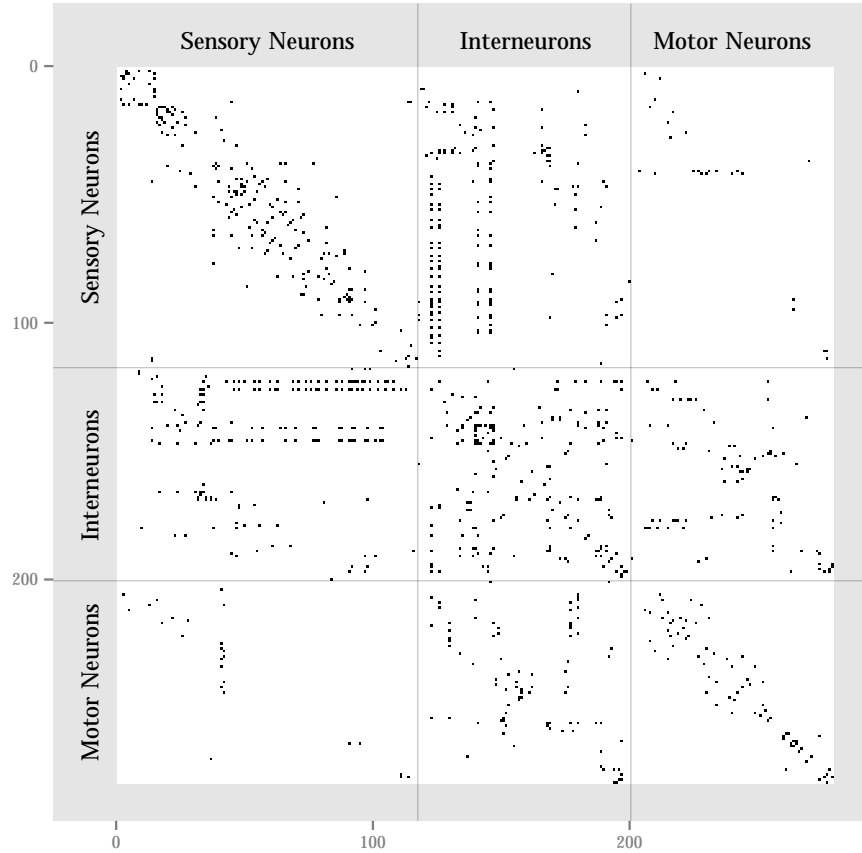


Figure 5: The adjacency matrix for the *C. elegans* connectome. The graph has 279 vertices and 515 edges. Black pixels indicate the presence of an edge and white pixels indicate no edge is present. The vertical and horizontal lines divide the adjacency matrix according to the three types of neurons.

as q increases the overall cost increases allowing for higher quality classification for the same quantity of edge assessment. We assume that the accuracy is identical for edges and non-edges which may at first appear as a simplification but as non-assessed edges are automatically assigned as non-edges this assumption is without loss of generality.

To investigate the trade-off phenomena, we simulated errorful observations of the connectome for various values of these parameters and computed the leave-one-out classification error using the Bayes plug-in classifier in Eq. (6). The results are displayed in Figure 6. Each filled area in the figure corresponds to one selection of the two parameters and the color indicates the mean leave-one-out classification error rate based on 1000 Monte Carlo replicates. In the x, y coordinates of figure, ie the edge-assessment-probability, edge-

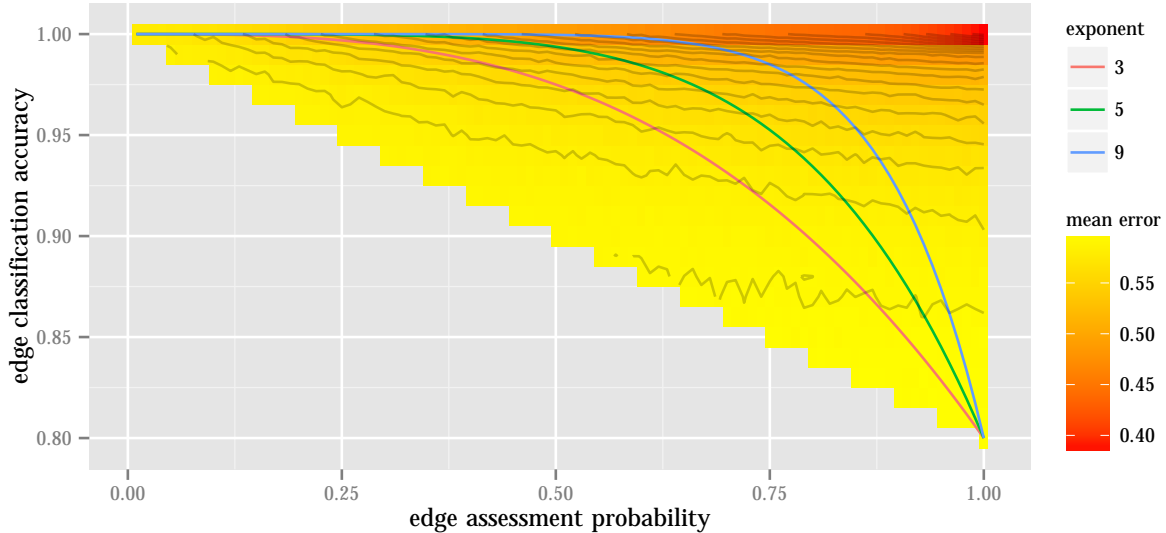


Figure 6: Each “pixel” in the figure corresponds to one selection of the edge assessment probability and edge classification accuracy for an errorful observation of the *C. elegans* connectome. The color indicates the mean leave-one-out classification error rate based on 1000 Monte Carlo replicates using the SBM Bayes plugin classifier. As expected, the error rate decreases substantially as both parameters increase. The three curves depict three possible profiles for a quality/quantity trade-off between the two parameters. Figure 7 shows the mean error rates along these three curves.

classification-accuracy coordinates, the point $(1, 1)$ corresponds to perfect observation of the graph, the line $x = 0$ corresponds to assessing zero edges and the line $y = 0.5$ (not shown in the figure) corresponds to sampling an Erdős-Rényi graph in which non-trivial error rates are impossible. As expected, the error rate decreases substantially as both parameters increase.

To further illustrate the quantity/quality trade-off phenomenon we considered three different curves through the space of the parameters given by the equation $y = 1 - 0.2x^q$ where x is the edge assessment probability $h(\kappa)$, y is the edge classification accuracy conditional on assessment, and $q \in \{3, 5, 9\}$. These curves are shown in Figure 6 in red, green, and blue. Note that as q increases the edge classification accuracy decreases more slowly when the edge assessment probability is small but then decreases more rapidly when the edge assessment probability is large. In our notation, higher values of q represent less rapidly decreasing functions h . This represents different degrees of the quality/quantity trade-off that may be present based on various experimental contexts.

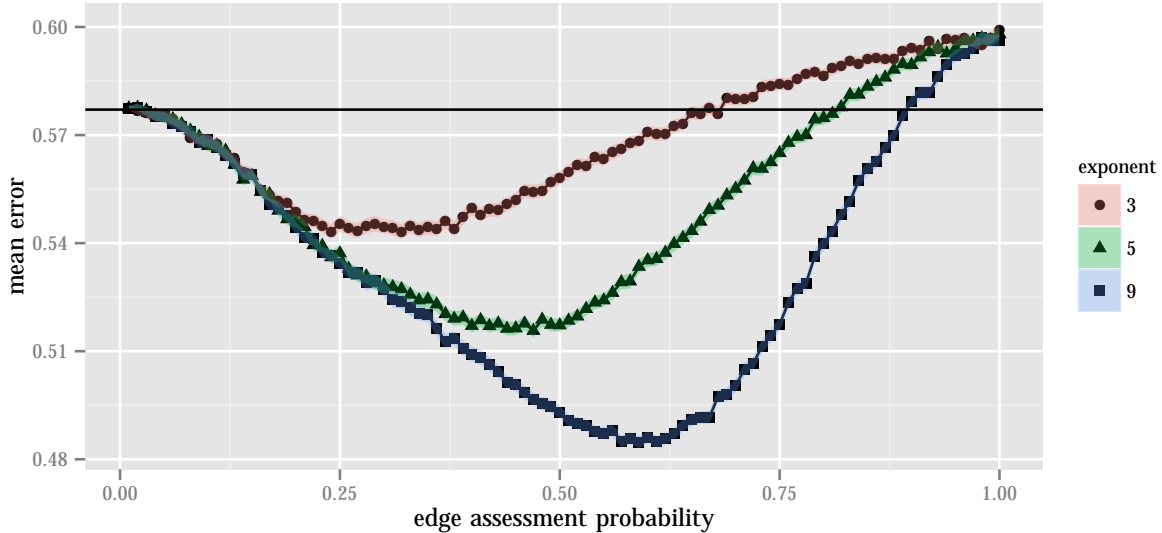


Figure 7: The three curves indicate the mean leave-one-out error rate for vertex classification based on an errorful observation of the *C. Elegans* connectome as the edge assessment probability varies with edge classification accuracy given by the equation $y = 1 - 0.2x^q$ for $q \in \{3, 5, 9\}$ (see Figure 6). The three exponents represent different degrees of the quality/quantity tradeoff and we demonstrate that the optimal operating point and resulting performance depends on this exponent. The horizontal black line indicates the chance error rate for the vertex classification task.

In Figure 7, the mean leave-one-out error rates for the three curves are shown with each point again corresponding to 1000 Monte Carlo replicates. The colored shaded areas indicate the 95% confidence intervals for the mean leave-one-out error rates. These curves indicate that the different values of the exponent and hence different quality/quantity trade-off regimes lead to different optimal operating points and ultimate inference task performance. This investigation illustrates that the quantity quality trade-off phenomenon will be present even in cases that deviate substantially from the idealized setting of this paper.

5 Conclusions

We have presented a simple model for errorfully observed graphs derived from classifying potential edges based on observed edge-features. For this model, we have investigated optimal vertex classification in the face of the quantity/quality trade-off: more informative edge-features are more expensive, and hence the

number of potential edges that can be assessed decreases with the quality of the edge-features. Considering a simple vertex classification rule, we have derived the optimal quantity/quality operating point and demonstrated that the Bayes optimal edge-classifier is not necessarily the optimal choice of edge-classifier for the subsequent graph inference task. In this section we will briefly investigate various extensions and alternative considerations to the setting presented thus far.

5.1 Large Sample Approximation

For sufficiently large n , the Binomial distributions that appear in Eq. (3) can be approximated by normal distributions: $\text{Bin}(n_k, \tilde{B}_{kk'}) \approx \mathcal{N}(n_k \tilde{B}_{kk'}, n_k \tilde{B}_{kk'}(1 - \tilde{B}_{kk'}))$. In the simplified regime of Section 4.1, we have conditioned on the fact that among the n vertices with observed class labels, exactly $n/2$ are in each of the two classes and we assume $B_{11} = B_{22} > B_{12}$ resulting in the simplified form of the error rate in Eq. (5). We recall that the number of observed edges from vertex v^* to block k' is $D_k(v^*)$ which condition on $Y(v^*) = k$ is distributed as $\text{Bin}(n_k, \tilde{B}_{kk'})$. In this setting, the classifier in Eq. (4) is Bayes optimal and the normal approximation to the binomial gives that, conditional on $Y(v^*) = k$, the difference $D_2(v^*) - D_1(v^*)$ has approximate distribution

$$\mathcal{N}\left((-1)^k \frac{n}{2}(\tilde{B}_{11} - \tilde{B}_{12}), \frac{n}{2}(\tilde{B}_{k2}(1 - \tilde{B}_{k2}) + \tilde{B}_{k1}(1 - \tilde{B}_{k1}))\right). \quad (7)$$

We can use this to approximate the error rate $L_{\kappa, \tau}$ as $L_{\kappa, \tau}^{\mathcal{N}} = \Phi(-\mu/\sigma)$, where Φ is the cumulative distribution function for a standard normal and μ and σ are the mean and standard deviation from Eq. (7). As $L_{\kappa, \tau}^{\mathcal{N}}$ decreases as μ/σ increases, the following simplified procedure for selecting τ and κ can be used:

$$\begin{aligned} (\kappa^{\mathcal{N}}, \tau^{\mathcal{N}}) &= \underset{\kappa, \tau}{\operatorname{argmax}} \quad \mu/\sigma \\ \text{where } \mu &= \frac{n}{2}(\tilde{B}_{11} - \tilde{B}_{12}), \\ \sigma^2 &= \frac{n}{2}(\tilde{B}_{k2}(1 - \tilde{B}_{k2}) + \tilde{B}_{k1}(1 - \tilde{B}_{k1})) \end{aligned}$$

and the 2×2 matrix \tilde{B} is given by Eq. (1). A comparison of the black solid line and greed dashed line in Figure 8 illustrates the accuracy of using this approximation for selecting τ when κ is fixed.

5.2 Minimizing Projection Error

Spectral embedding methods proceed by finding a low-rank latent space representation (projection). In the case of $SBM([n], B, \pi)$ with $\operatorname{rank}(B) = d$, standard results from perturbation analysis (e.g., [Davis and](#)

Kahan (1970)) demonstrate that $(\kappa^{\mathcal{P}}, \tau^{\mathcal{P}}) = \arg \min_{\kappa, \tau} \max_k (\pi \tilde{B})_k / \lambda_d^2$, where the numerator $(\pi \tilde{B})_k$ is the k^{th} element of the K -vector $(\pi \tilde{B})$ and the denominator λ_d^2 is the square of the d^{th} largest eigenvalue of the $K \times K$ matrix $(\text{diag}(\pi) \tilde{B})$, minimizes (with high probability) an upper bound on the projection error. We leave further investigations of this kind as future work and note that for our simple demonstration case, this approach is equivalent to our large sample approximation $(\kappa^{\mathcal{N}}, \tau^{\mathcal{N}})$.

5.3 The Surrogate is Instructive

The vertex classification methodology we have investigated is perhaps the simplest nontrivial approach. In particular, we have so far shirked any methodology based on the common approach to general graph inference of first embedding the graph into finite-dimensional Euclidean space and then addressing inference therein. The reason for this is a clear self-indictment: we are so far mostly unable to directly analyze the quantity/quality trade-off for statistical inference on errorfully observed graphs in any such methodology (except by resorting to the asymptotic implications of a limit theorem in Athreya et al. (2013)).

We do, however, have a wealth of empirical evidence suggesting that our surrogate optimization yields results that can be profitably used to choose the (κ, τ) quantity/quality operating point for these “inference composed with embedding” methodologies. Figure 8 presents one illustrative empirical result supporting this claim. Figure 8 is obtained as follows. For our demonstration setting in § 4.1, we employ the adjacency-spectral embedding (Sussman et al., 2012) to embed the vertices of a graph into points in \mathbb{R}^2 (see also Figure 1). The results in Sussman et al. (2013); Tang et al. (2013) indicate that the resulting embedding is conducive for subsequent inference, i.e., under the latent position model of § 1.1, the embeddings of the vertices converge, in the limit as $n \rightarrow \infty$, to the latent positions. We then use Fisher’s Linear Discriminant (Duda and Hart, 1973) for the two-class classification in \mathbb{R}^2 to classify the vertices. The result, for our demonstration setting with $\kappa^* = 3.5$ is given in Figure 8. For any fixed (κ, τ) , Monte Carlo yields the estimate $\hat{L}_{\kappa, \tau}^{\mathcal{P}}$ of probability of misclassification. The number of Monte Carlo replicates for each choice of κ and τ is 10000.

The blue curve in Figure 8 is a theoretical version of the red dots based on recent results of Athreya et al. (2013). The results in Sussman et al. (2013); Tang et al. (2013) are in a sense first order results in that they demonstrated only that the embeddings converge, in the limit, to the latent positions. Athreya et al. (2013) strengthen these first order results and by showing that for sufficiently large n , the embedding position of a vertex v is approximately distributed according to a multivariate normal with mean $Z(v)$, the latent position associated with v , and covariance matrix $\Sigma(v)$, with $\Sigma(v)$ converging to 0 at the rate

of $\Theta(1/\sqrt{n})$. For a general $K \times K$ stochastic blockmodel where each block corresponds to a class label, this means that the embedding of a vertex v with class label $k \in \{1, 2, \dots, K\}$ is distributed multivariate normal with mean $\mu^{(k)} \in \mathbb{R}^d$ and covariance matrix $\Sigma^{(k)} \in \mathbb{R}^{d \times d}$ where d , the rank of the matrix B , is the embedding dimension. Therefore, operating in the asymptotic regime, our quantity/quality trade-off corresponds to finding the κ, τ that minimizes the error when classifying points that are distributed as a mixture of multivariate Gaussians $\sum_k \pi_k \phi_{\text{MVN}}(\mu_{\kappa, \tau}^{(k)}, \Sigma_{\kappa, \tau}^{(k)})$ where $\mu_{\kappa, \tau}^{(k)}$ and $\Sigma_{\kappa, \tau}^{(k)}$ can be computed explicitly, for any given B and any choice of the κ and τ parameters. The Bayes optimal vertex classifier, as suggested by the conjecture, corresponds to a comparison of the densities under this multivariate normal assumption. The blue curve in Figure 8 is therefore the plot of the theoretical version of the red dots in Figure 8, where instead of performing Fisher’s Linear Discriminant for many Monte Carlo replicates, we compute the error rate for Fisher’s Linear Discriminant based on the conjectured theoretical means and theoretical covariance matrices. The formulae for the covariance matrices are given in [Athreya et al. \(2013\)](#). The resulting error rate is much lower than our other methods because the number of vertices is not large enough so that the asymptotic normal approximation is accurate. On the other hand it is valuable to note that the optimal τ provided by this method is close to the optimal τ provided by our other methods.

5.4 The “Missing” Model

The formulation we presented in Section 2 for errorfully observed graphs $\tilde{\mathbb{G}} \sim \text{SBM}([n], \tilde{B}, \pi)$ assumes that the potential edges not classified at all, due to the quality penalty $h(\kappa)$, are set to 0 – i.e., non-edge. In fact, in many use cases we might expect to have full knowledge of which potential edges have been classified as non-edges and which potential edges have not been classified at all, and it seems sensible to treat these latter as “missing.” (Recall that we assume that the potential edges not classified at all are MCAR.)

This “missing” model is specified as in Section 2, but with two important alterations. First, while $\tilde{B} = h(\kappa) [(1 - F_{1, \kappa}(\tau))B + (1 - F_{0, \kappa}(\tau))(J - B)]$, we consider $\tilde{B}_{\text{MCAR}} = (1 - F_{1, \kappa}(\tau))B + (1 - F_{0, \kappa}(\tau))(J - B)$. That is, the quality penalty $h(\kappa)$ does *not* impact the errorful block connectivity probability matrix \tilde{B}_{MCAR} . Then we consider $\tilde{\mathbb{G}}_{\text{MCAR}} \sim s_{h(\kappa)} \left(\text{SBM}([n], \tilde{B}_{\text{MCAR}}, \pi) \right)$, where $s_p(F_{\mathbb{G}})$ for $p \in [0, 1]$ and for some graph distribution $F_{\mathbb{G}}$ indicates random sampling of potential edges; the potential edges not sampled through s_p are left as missing entries in the adjacency matrix A . (Contrast this with the notionally similar $\text{SBM}([n\sqrt{h(\kappa)}], \tilde{B}, \pi)$.)

This “missing” model can then be analyzed through the perspective of imputations and inference with missing data. The literature on statistical analysis with missing data is vast, see e.g., [Little and Rubin](#)

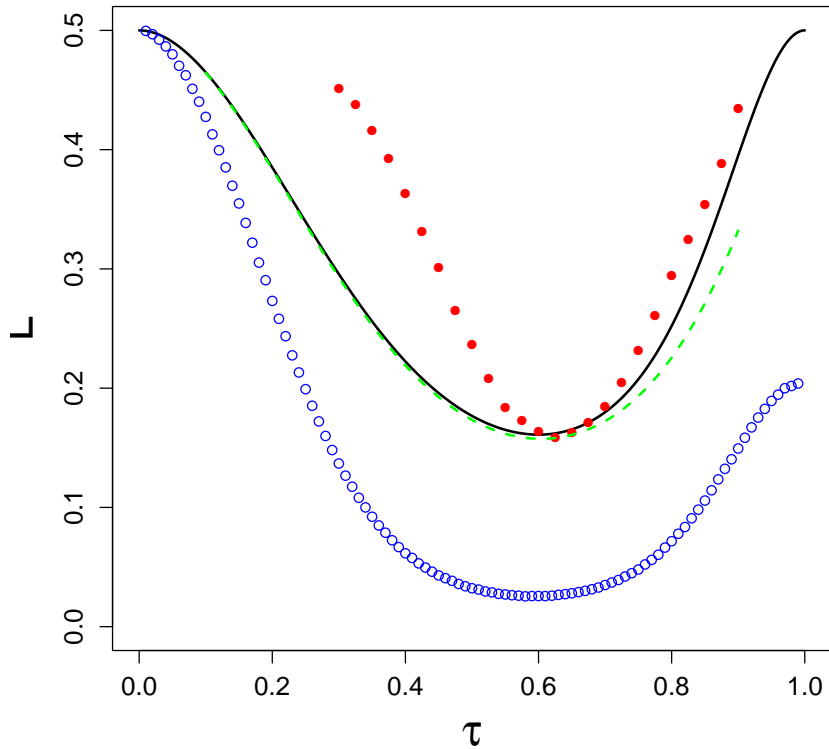


Figure 8: For our demonstration setting with $\kappa^* = 3.5$, we see that the surrogate optimization is instructive regarding more elaborate graph inference: the black solid curve is analytic $L_{\kappa^*, \tau}$, the Bayes; the green dashed curve is the large sample normal approximation $L_{\kappa^*, \tau}^{\mathcal{N}}$; the blue curve is the error rate of Fisher's Linear Discriminant for points distributed according to the asymptotic mixture of multivariate normal distributions of the embedded points from [Athreya et al. \(2013\)](#); the red dotted curve is Monte Carlo $\widehat{L}_{\kappa^*, \tau}^{\mathcal{P}}$ (NB: the standard errors for the Monte Carlo are so small they are hidden within the red dots). Result: $\tau_{Bayes} \approx 1/2$; $\tau^* \approx 0.600$; $\tau^{\mathcal{N}} \approx 0.604$; $\tau^{\mathcal{P}} \approx 0.610$.

(2002); Reiter and Raghunathan (2007); Rubin (1996). In what follows, we discuss briefly the analysis of this missing model and its relationship with our quantity/quality trade-off as discussed earlier in the paper. Our discussion is somewhat cursory, as a detailed investigation is difficult in the scope of the paper.

We can consider the random graph $\tilde{\mathbb{G}}$ as analyzed previously in the paper to be an instantiation of $\tilde{\mathbb{G}}_{MCAR}$ with the missing values imputed to be 0s (non-edges). For $\tilde{\mathbb{G}}_{MCAR}$, if we assume that the entries of the matrix \tilde{B} are known, then the Bayes optimal vertex classifier is given as follows. For a vertex v , classify v as being of class 1 or 2 depending on whether the ratio

$$\frac{\tilde{B}_{11}^{m_1} (1 - \tilde{B}_{11})^{o_1 - m_1} \tilde{B}_{12}^{m_2} (1 - \tilde{B}_{12})^{o_2 - m_2}}{\tilde{B}_{21}^{m_1} (1 - \tilde{B}_{21})^{o_1 - m_1} \tilde{B}_{22}^{m_2} (1 - \tilde{B}_{22})^{o_2 - m_2}}$$

is larger or smaller than 1, where o_1 and o_2 are the number of potential edges from v to the n_1 and n_2 vertices of classes 1 and 2 that were classified by the edge classifier, respectively. We then obtain analogous optimization results to those presented in Section 4 above. In particular, for large $n_1 = n_2$, the likelihood in both the numerator and denominator of the above ratio are concentrated around $o_1 \approx nh(\kappa)/2$, $o_2 \approx nh(\kappa)/2$ ($n = n_1 + n_2$) and so the above likelihood ratio corresponds roughly to our simple vertex classifier in § 4.1. In particular, for $\tilde{\mathbb{G}}_{MCAR}$ we obtain analogous optimization results to those presented in Section 4 above. However, in general, as the entries of the matrix \tilde{B} are unknown and need to be estimated from the data, the Bayes optimal vertex classifier for $\tilde{\mathbb{G}}_{MCAR}$ is not as simple as our vertex classifier γ in § 4.1.

In summary, for our quantity/quality trade-off framework, the difference between a complete case analysis based on labeling the missing values as “NA” versus analysis wherein we impute the missing values to be 0s (non-edges) is negligible. Of fundamental interest is therefore the quantity/quality optimization for more elaborate imputation schemes.

5.5 Discussion

Alas, we do not know the block connectivity probability matrix \tilde{B} or block probability vector π . (And of course we are not really facing a stochastic blockmodel ... but in many applications – for example, connectomics and social networks – a stochastic blockmodel can be a productive (if overly simple) first model.) We note that, for a given κ , one can obtain estimates of \tilde{B} and π from the available $\{X(uv)\}$ and $\{Y(v)\}$, assuming a parametric form for the class-conditional edge-feature distributions $F_{0,\kappa}$ and $F_{1,\kappa}$. Nevertheless, our primary purpose has been to present a foundational analysis of the quantity/quality trade-off for errorfully observed graphs and to demonstrate the folly of fixating on the optimization of the edge-classifier for edge-classification performance when subsequent graph inference is the ultimate goal.

Appendix

Connectomics

Connectomics is a burgeoning field in which investigators estimate brain-graphs (connectomes) for subsequent inference tasks. For example, Electron Microscopy (EM) connectomics investigations explore hypotheses of conditional independence between vertices (Bock et al., 2011), and Magnetic Resonance (MR) connectomics often use brain-graphs as biomarkers for phenotypic variability (Vogelstein et al., 2013). Regardless of the experimental modality or subsequent inference task, connectomics investigators *always* face quantity/quality trade-offs with regard to graph inference. These trade-offs arise in at least two stages of the analytics pipeline: (1) data collection, (2) data analysis. In particular, in EM connectomics, different experimental paradigms admit different spatial resolutions for the same imaging time (Briggman and Bock, 2012), yielding a number of distinct κ 's. Regardless of the chosen imaging modality, manual, semi- or fully-automatic tracing algorithms are then employed to infer the graph from the noisy image data (Briggman and Denk, 2006). Each edge, therefore, can be endowed with a confidence level, which corresponds to the edge-features of interest described above. Similarly, in MR connectomes, different scanner sequences yield higher spatial resolution, but therefore reduce the signal-to-noise ratio per voxel (Haacke et al., 1999). Given the noisy MR connectomics data, “tractography” algorithms estimate connectivity amongst brain voxels (Gray et al., 2010). Again, each edge can be endowed with a confidence. Historically, for any connectomics investigation, the threshold for counting an edge as “real” has been ad hoc, at best. Priebe et al. (2012) presents a first principled treatment of this issue. This manuscript suggests that we can choose both τ and κ to optimize our subsequent inference task.

Social Networks

Social network analysis is another burgeoning field in which the data are represented via a graph. In this setting, vertices (actors) represent individuals and edges (links or ties) typically represent communication between pairs of actors. A classic example is the Enron email graph (Priebe et al., 2005). For these data, we place an edge between a pair of actors according to whether an email was exchanged between the pair. Both the vertices and edges can be endowed with complex attributes. For example, edges may be attributed with a word-count vector, in which each dimension corresponds to a unique word. The dimensionality of these attributes, however, is exceedingly large.

We can reduce the edge attribute dimensionality via topic modeling (Blei et al., 2003; Deerwester et al., 1990;

Papadimitriou et al., 2000). Topic models learn a set of “topics” associated with each document (in this case, an email message). Topic modeling objective functions also tend to be computationally demanding. Therefore, a number of approximations are typically employed to obtain approximately optimal solutions that scale up to very large data, including variants of online variational Bayes (Hoffman et al., 2010), stochastic gradient descent (Mimno et al., 2012), latent factor modeling (Zhou et al., 2012) and parallelization schemes (Ahmed et al., 2012). Each of these approaches makes important approximation/computation trade-offs, which are not currently understood very well (Asuncion et al., 2009) – especially in terms of subsequent inference.

Recalling the Enron email example, we may be interested in inference based on only those email messages with certain key topics, such as sports (or insider trading). But assessing which emails contain the interactions of interest is a “Human Language Technology” (HLT) problem. The computational trade-offs associated with MCMC and variational Bayesian methods, for example, induces a quantity/quality trade-off for assigning edge features. Specifically, we can invest more or less HLT time per edge, from manual investigation (humans reading the messages) to simple keyword search: more expensive HLT will yield more accurate topic estimation, but at the cost of fewer messages assessed, while less expensive HLT will yield less accurate topic estimation, but for a larger number of messages assessed. The ability to determine the optimal operating point for this quantity/quality trade-off for a given computational budget will lead to superior subsequent inference for a wide variety of social network analysis tasks.

Acknowledgments

This work is partially funded by the National Security Science and Engineering Faculty Fellowship (NSSEFF), the Johns Hopkins University Human Language Technology Center of Excellence (JHU HLT COE), and the XDATA program of the Defense Advanced Research Projects Agency (DARPA) administered through Air Force Research Laboratory contract FA8750-12-2-0303. We also thank the editors and the anonymous referees for their valuable comments and critiques that greatly improved this work.

References

- A. Ahmed, M. Aly, J. Gonzalez, S. Narayanamurthy, and A. Smola. Scalable inference in latent variable models. In *Proceedings of the 2012 ACM International Conference on Web Search and Data Mining*, pages 123–132, 2012.

- E.M. Airoldi, D.M. Blei, S.E. Fienberg, and E.P. Xing. Mixed membership stochastic blockmodels. *Journal of Machine Learning Research*, 9:1981–2014, 2008.
- A. Asuncion, M. Welling, P. Smyth, and Y. W. Teh. On smoothing and inference for topic models. In *Proceedings of the 2009 Conference on Uncertainty in Artificial Intelligence*, pages 27–34, 2009.
- A. Athreya, V. Lyzinski, D. J. Marchette, C. E. Priebe, D. L. Sussman, and M. Tang. A limit theorem for scaled eigenvectors of random dot product graphs. Arxiv preprint. <http://arxiv.org/abs/1305.7388>, 2013.
- M. Belkin and P. Niyogi. Laplacian eigenmaps for dimensionality reduction and data representation. *Neural Computation*, 15:1373–1396, 2003.
- D. M. Blei. Probabilistic topic models. *Communications of the ACM*, 55:77–84, 2012.
- D.M. Blei, A.Y. Ng, and M.I. Jordan. Latent Dirichlet allocation. *Journal of Machine Learning Research*, 3:993–1022, 2003.
- D.D. Bock, Wei-Chung A. Lee, A.M. Kerlin, M.L. Andermann, A.W. Wetzell, S. Yurgenson, E.R. Soucy, H.S. Kim, G. Hood, and R.C. Reid. Network anatomy and in vivo physiology of visual cortical neurons. *Nature*, 471(7337):177–182, 2011.
- V. Braitenberg and A. Schüz. *Anatomy of the cortex: statistics and geometry*. Springer, Berlin, Germany, 1991. ISBN 3-540-53233-1.
- K.L. Briggman and D.D. Bock. Volume electron microscopy for neuronal circuit reconstruction. *Current opinion in neurobiology*, 22(1):154–61, 2012.
- K.L. Briggman and W. Denk. Towards neural circuit reconstruction with volume electron microscopy techniques. *Current opinion in neurobiology*, 16(5):562–70, 2006.
- C. Davis and W. Kahan. The rotation of eigenvectors by a perturbation. III. *Siam Journal on Numerical Analysis*, 7:1–46, 1970.
- S. Deerwester, S.T. Dumais, G.W. Furnas, T.K. Landauer, and R. Harshman. Indexing by latent semantic analysis. *Journal of the American Society for Information Science*, 41(6):391–407, 1990.
- L. Devroye, L. Györfi, and G. Lugosi. *A Probabilistic Theory of Pattern Recognition*. Springer Verlag, 1996.
- R. O. Duda and P. E. Hart. *Pattern Classification and Scene Analysis*. John Wiley & Sons, New York, 1973.

- D. E. Fishkind, D. L. Sussman, M. Tang, J.T. Vogelstein, and C.E. Priebe. Consistent adjacency-spectral partitioning for the stochastic block model when the model parameters are unknown. *SIAM Journal on Matrix Analysis and Applications*, 34:23–39, 2013.
- W.R. Gray, J.A. Bogovic, J.T. Vogelstein, B.A. Landman, J.L. Prince, and R.J. Vogelstein. Magnetic resonance connectome automated pipeline: an overview. *IEEE pulse*, 3(2):42–8, March 2010.
- E. Mark Haacke, Robuert W. Bornw, Michael R. Thompson, and Ramesh Venkatesan. *Magnetic Resonance Imaging: Physical Principles and Sequence Design*. Wiley-Liss, 1999.
- P. Hoff, A. Rafferty, and M. Handcock. Latent space approaches to social network analysis. *Journal of the American Statistical Association*, 97:1090–1098, 2002.
- M.D. Hoffman, D.M. Blei, and F. Bach. Online learning for latent Dirichlet allocation. *Advances in Neural Information Processing Systems*, 23:856–864, 2010.
- P.W. Holland, K. Laskey, and S. Leinhardt. Stochastic blockmodels: First steps. *Social Networks*, 5(2): 109–137, 1983.
- R. J. A. Little and D. B. Rubin. *Statistical Analysis with missing data*. John Wiley and Sons, 2002.
- D. Mimno, M.D. Hoffman, and D.M. Blei. Sparse stochastic inference for latent Dirichlet allocation. In *Proceedings of the 2012 International Conference on Machine Learning*, 2012.
- C.H. Papadimitriou, P. Raghavan, H. Tamaki, and S. Vempala. Latent semantic indexing: A probabilistic analysis. *Journal of Computer and System Sciences*, 61:217–235, 2000.
- C.E. Priebe, J.M. Conroy, D.J. Marchette, and Y. Park. Scan statistics on enron graphs. *Computational & Mathematical Organization Theory*, 11(3):229–247, 2005.
- C.E. Priebe, J.T. Vogelstein, and D.D. Bock. Optimizing the quantity/quality trade-off in connectome inference. *Communications in Statistics - Theory and Methods (in press)*, 2012.
- J. P. Reiter and T. E. Raghunathan. The multiple adaptations of multiple imputation. *Journal of the American Statistical Association*, 102:1462–1471, 2007.
- D. B. Rubin. Multiple imputation after 18+ years. *Journal of the American Statistical Association*, 91: 473–489, 1996.
- T. A. B. Snijders and K. Nowicki. Estimation and Prediction for Stochastic Blockmodels for Graphs with Latent Block Structure. *Journal of Classification*, 14(1):75–100, 1997.

- D. L. Sussman, M. Tang, D. E. Fishkind, and C. E. Priebe. A consistent adjacency spectral embedding for stochastic blockmodel graphs. *Journal of the American Statistical Association*, 107(499):1119–1128, 2012.
- D. L. Sussman, M. Tang, and C.E. Priebe. Consistent latent position estimation and vertex classification for random dot product graphs. *IEEE Transactions on Pattern Analysis and Machine Intelligence*, 2013. In press.
- M. Tang, D. L. Sussman, and C. E. Priebe. Universally consistent vertex classification for latent position graphs. *Annals of Statistics*, 31:1406–1430, 2013.
- L. R. Varshney, B. L. Chen, E. Paniagua, D. H. Hall, and D. B. Chklovskii. Structural properties of the *Caenorhabditis elegans* neuronal network. *PLoS Comput. Biol.*, 7(2), 2011.
- J.T. Vogelstein, W.R. Gray, R.J. Vogelstein, and C.E. Priebe. Graph Classification using Signal Subgraphs: Applications in Statistical Connectomics. *IEEE Transactions on Pattern Analysis and Machine Intelligence*, 35:1539–1551, 2013.
- Y.J. Wang and G.Y. Wong. Stochastic Blockmodels for Directed Graphs. *Journal of the American Statistical Association*, 82(397):8, March 1987.
- J.G. White, E. Southgate, J.N. Thomson, and S. Brenner. The structure of the nervous system of the nematode *Caenorhabditis elegans*. *Philosophical Transactions of the Royal Society of London. B, Biological Sciences*, 314(1165):1–340, 1986.
- S. Young and E. Scheinerman. Random dot product models for social networks. In *Proceedings of the 5th international conference on algorithms and models for the web-graph*, pages 138–149, 2007.
- M. Zhou, L. Hannah, D. Dunson, and L. Carin. Beta-negative binomial process and poisson factor analysis. In *Proceedings of the Fifteenth International Conference on Artificial Intelligence and Statistics*, pages 1462–1471, 2012.